the plant journal

SEB Society for Experimental Biology

The Plant Journal (2014) **77,** 146–159 doi: 10.1111/tpj.12374

Rhizobial infection does not require cortical expression of upstream common symbiosis genes responsible for the induction of Ca^{2+} spiking

Teruyuki Hayashi[1,†], Yoshikazu Shimoda[1], Shusei Sato[2,‡], Satoshi Tabata[2], Haruko Imaizumi-Anraku[1,*] and Makoto Hayashi[1]

[1]*Division of Plant Sciences, National Institute of Agrobiological Sciences, 2–1–2 Kannon–dai, Tsukuba 305–8602, Japan, and* [2]*Kazusa DNA Research Institute, 2–6–7 Kazusa-kamatari, Kisarazu, Chiba 292–0818, Japan*

Received 16 July 2013; revised 15 October 2013; accepted 29 October 2013; published online 7 November 2013.
*For correspondence (e-mail onko@affrc.go.jp).
†Present address: Graduate School of Biological Sciences, Nara Institute of Science and Technology, 8916–5 Takayama–cho, Ikoma, Nara 630–0192, Japan.
‡Present address: Graduate School of Life Sciences, Tohoku University, 2–1–1 Katahira, Aoba–ku, Sendai 980–8577, Japan.

SUMMARY

For the establishment of an effective root nodule symbiosis, a coordinated regulation of the infection processes between the epidermis and cortex is required. However, it remains unclear whether the symbiotic genes identified so far are involved in epidermal and/or cortical infection, e.g. epidermal and cortical infection thread formation or cortical cell division. To analyze the symbiotic gene requirements of the infection process, we have developed an epidermis-specific expression system (*pEpi* expression system) and examined the symbiotic genes *NFR1*, *NFR5*, *NUP85*, *NUP133*, *CASTOR*, *POLLUX*, *CCaMK*, *CYCLOPS*, *NSP1* and *NSP2* for involvement in the infection process in the epidermis and cortex. Our study shows that expression of the upstream common symbiosis genes *CASTOR*, *POLLUX*, *NUP85* and *NUP133* in the epidermis is sufficient to induce formation of infection threads and cortical cell division, leading to the development of fully effective nodules. Our system also shows a requirement of *CCaMK*, *CYCLOPS*, *NSP1* and *NSP2* for the entire nodulation process, and the different contributions of *NFR1* and *NFR5* to cortical infection thread formation. Based on these analyses using the *pEpi* expression system, we propose a functional model of symbiotic genes for epidermal and cortical infection.

Keywords: *Lotus japonicus*, root nodule symbiosis, infection threads, cortical cell division, root epidermis, root cortex, epidermis-specific expression system (*pEpi* expression system).

INTRODUCTION

Leguminous plants have the ability to establish endosymbiosis with soil bacteria (collectively termed rhizobia), and form root nodules in which rhizobia fix atmospheric nitrogen (Kouchi *et al.*, 2010). Recent studies of symbiotic mutants of the model legumes *Lotus japonicus* and *Medicago truncatula* have led to the identification of a number of host genes that regulate root nodule and/or arbuscular mycorrhizal symbioses (Parniske, 2008). In *L. japonicus*, two LysM receptor-like kinases, NFR1 and NFR5, are essential for specific recognition of Nod factors secreted from *Mesorhizobium loti* (Madsen *et al.*, 2003; Radutoiu *et al.*, 2003). Downstream of these receptors, a leucine-rich repeat receptor kinase (SYMRK; Stracke *et al.*, 2002), three components of the nucleopore (NUP133, NUP85 and NENA; Kanamori *et al.*, 2006; Saito *et al.*, 2007; Groth *et al.*, 2010), two cation channel proteins (CASTOR and POLLUX; Ané *et al.*, 2004; Imaizumi-Anraku *et al.*, 2005), Ca^{2+}/calmodulin-dependent protein kinase (CCaMK; Lévy *et al.*, 2004; Gleason *et al.*, 2006; Tirichine *et al.*, 2006) and a coiled-coil domain-containing protein (CYCLOPS; Yano *et al.*, 2008) have been identified as components of the 'common symbiosis pathway' that is required for both root nodule and arbuscular mycorrhizal symbioses. Following the perception of Nod factors through NFR1 and NFR5, Ca^{2+} influx at the tip of the root hair and Ca^{2+} spiking at the perinuclear region of the root hair are induced. Among the eight common symbiosis pathway genes, *SYMRK*, *NUP85*, *NUP133*, *NENA*, *CASTOR* and *POLLUX* are essential for the generation of Ca^{2+} spiking in response to Nod factors (Miwa *et al.*, 2006; Groth *et al.*, 2010). Therefore, these symbiotic genes are denoted as 'upstream genes' of the common symbiosis pathway (Hayashi *et al.*, 2010). In contrast, *CCaMK* and

CYCLOPS are positioned downstream of Ca^{2+} spiking (Miwa *et al.*, 2006). Two GRAS family transcription factor genes (*NSP1* and *NSP2*; Kaló *et al.*, 2005; Smit *et al.*, 2005; Heckmann *et al.*, 2006; Murakami *et al.*, 2006) and a putative transcription factor gene (*NIN*, Schauser *et al.*, 1999) are located downstream of Ca^{2+} spiking (Miwa *et al.*, 2006), and are necessary for both nodule organogenesis and rhizobial infection, accompanied by the formation of infection threads (ITs).

Mutational perturbation of the symbiotic genes mentioned above leads to severe impairment of IT formation in root hairs. Thus, the majority of symbiotic mutants have a non-nodulation phenotype, suggesting that these symbiotic genes function at least in the root epidermis, but the role of these genes in cortical IT formation and cortical cell division remains unclear. However, in the case of the *symrk–14* and *nena–1* mutants, although epidermal IT formation is impaired, cortical IT formation and cortical cell division occur, resulting in the formation of effective nodules (Groth *et al.*, 2010; Kosuta *et al.*, 2011). In contrast, although epidermal IT formation occurs, arrested development of cortical ITs was observed in *ccamk–14* mutant (Liao *et al.*, 2012), making it difficult to understand the functionality of those symbiotic genes in both the epidermis and cortex. Functional analyses of symbiotic genes, using a combination of loss-of-function mutants transformed with gain-of-function CCaMK or LHK1 (which encodes a cytokinin receptor kinase), have revealed regulation pathways for both nodule organogenesis (Gleason *et al.*, 2006; Tirichine *et al.*, 2006, 2007; Marsh *et al.*, 2007; Yano *et al.*, 2008) and rhizobial infection (Hayashi *et al.*, 2010; Madsen *et al.*, 2010). However, it remains uncertain whether expression of these genes in the epidermis or cortex or both is a prerequisite for the accommodation of rhizobia. Using the *pLeEXT* (epidermis) and *pCO2* (cortex) tissue-specific promoters, Rival *et al.* (2012) proposed a model for the control of nodule organogenesis by *NFP* and *DMI3*, orthologs of *NFR5* and *CCaMK*, respectively, in *M. truncatula* (Rival *et al.*, 2012). However, the involvement of other symbiotic genes for nodule organogenesis remains elusive, and the roles of the symbiotic genes in epidermal and cortical IT formation require clarification. In order to dissect the symbiotic cellular responses that occur in two cell layers, we isolated *Lotus* expansin genes that are expressed specifically in the root epidermis, and developed a root epidermis-specific expression system called the '*pEpi* expression system', which makes it possible to express a symbiotic gene in the epidermis. Using the *pEpi* expression system, we analyzed the requirements of the symbiotic genes *NFR1*, *NFR5*, *NUP85*, *NUP133*, *CASTOR*, *POLLUX*, *CCaMK*, *CYCLOPS*, *NSP1* and *NSP2*, for epidermal and cortical rhizobial infection and nodule organogenesis.

RESULTS

A root epidermis-specific expression system using the promoter region of *Lotus expansinA7* orthologs

To develop a root epidermis-specific expression system (*pEpi* expression system) in *L. japonicus*, we searched for *Lotus* orthologs of *expansinA7* (*AtEXPA7*), an expansin gene that is known to be expressed specifically in the root hair cells of Arabidopsis (Cho and Cosgrove, 2002). A BLAST search (http://blast.ncbi.nlm.nih.gov/Blast.cgi) using AtEXPA7 and AtEXPA18 as query sequences resulted in identification of two orthologs in *L. japonicus*. The amino acid sequence between 55 (Gly) and 181 (Ile) of AtEXPA7, and the corresponding regions of AtEXPA18, MtEXPA7, MtEXPA8 (Kim *et al.*, 2006) and *Lotus* expansin protein sequences were aligned using CLUSTALW (http://clustalw.ddbj.nig.ac.jp/) (Figure S1). Based on this phylogenetic tree, we named two *Lotus* expansin orthologs *LjEXPA7* and *LjEXPA8* [accession numbers AP010346 (region 34 276–34 741) and AP009544 (region 25 411–25 974), respectively]; these genes were closely related to *MtEXPA7* and *MtEXPA8*, respectively. To evaluate epidermis-specific expression of *LjEXPA* genes, root hairs of *Lotus* roots were isolated. The *RH101* and *RH102* genes, both of which have been reported to be expressed specifically in root hairs (Maekawa *et al.*, 2005), were highly expressed in the isolated root hairs in comparison with stripped roots that contain stele, cortex and epidermal cells but not root hairs (Figure S2). The *LjEXPA7* and *LjEXPA8* transcripts also showed a root hair-specific expression pattern (Figure 1a).

The promoter regions of *AtEXPA7* and *AtEXPA18* contain conserved root hair-specific *cis* elements (RHEs) that confer root hair-specific expression of expansins in angiosperms (Kim *et al.*, 2006). The RHE core consists of 16 or 17 nucleotides, and includes two conserved motifs, TG and CACG. As well as the *AtEXPA* genes, multiple RHEs were found in the promoter regions of both *LjEXPA7* and *LjEXPA8* (Figures 1b,c and S3). We selected three types of RHE-containing promoters, and tested their potential to drive root epidermis-specific expression of the β–glucuronidase gene (*GUSplus*; *GUS*$^{+}$) in *Lotus* roots (Figure 1d). *pEpi::GUS*$^{+}$ constructs were introduced by *Agrobacterium rhizogenes*-mediated hairy root transformation. GUS expression was observed mainly in epidermal cells and partially in the stele of transformed roots (Figure 1 g–l). In particular, *pEpi308*, which includes three RHEs, exhibited the most specific expression in epidermis (Figure 1i,j), and this epidermal expression was not affected by inoculation of *M. loti* (Figure S4). This is consistent with the fact that the abundance of the *LjEXPA7* transcript in root hairs was not changed in response to *M. loti* (Figure 1a). Thus we selected *pEpi308* for establishment of the *Epi* expression system. To avoid the possibility that gene expression

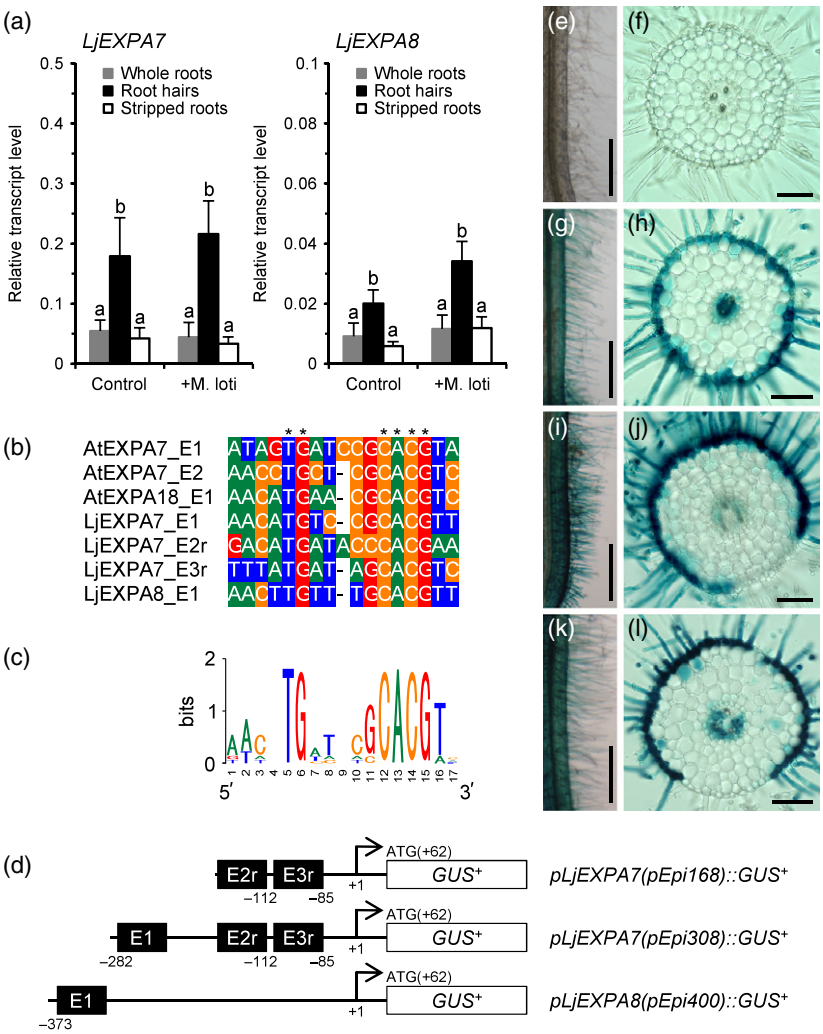

Figure 1. Root epidermis-specific expression system using promoter regions of AtEXPA7 orthologs in *Lotus*.
(a) Real-time RT–PCR analysis of *LjEXPA7* and *LjEXPA8* transcripts in root hairs, stripped roots or whole roots 2 days after mock inoculation (Control) or inoculation with *Mesorhizobium loti* (+*M. loti*). Values are means and SD of three or four biological replications. Bars with different letters are significantly different (Tukey–Kramer multiple comparison test, $P < 0.05$).
(b) Alignment of root hair-specific *cis* element (RHE) core sequences of promoter regions of EXPA orthologs. Asterisks indicate highly conserved nucleotides within the RHE core.
(c) Sequence logo representing the conservation of nucleotides at each position in the RHE cores. The sequence logo was generated using WebLogo (http://weblogo.berkeley.edu/).
(d) Illustrations of three types of RHE-containing promoter fused to the β-glucuronidase reporter gene (*GUSplus*; *GUS*$^+$). The numbers below the sequence are the starting nucleotide positions of the RHE core (black boxes). Nucleotide positions are numbered relative to the *att*R1 site of a Gateway destination vector cassette (the ATG start codon is at nucleotide positions 62–64). An '*r*' after the RHE number indicates a reverse orientation of the RHE.
(e–l) Promoter GUS analysis. *Lotus* roots were transformed with an empty vector (e, f), *pEpi168::GUS*$^+$ (g, h), *pEpi308::GUS*$^+$ (i, j) or *pEpi400::GUS*$^+$ (k, l) by *Agrobacterium rhizogenes*-mediated hairy root transformation. (f, h, j, l) Transverse sections of transformed roots. Scale bars = 500 μm (e, g, i, k) and 100 μm (f, h, j, l).

under the control of the *Epi* promoter interferes with rhizobial infection processes, we examined the rhizobial infection phenotypes on wild-type Gifu B–129 (wt) roots expressing *GUS*$^+$ under the control of the *pEpi* (wt/*pEpi::GUS*$^+$) or CaMV 35S promoter (wt/*p35S::GUS*$^+$). Upon inoculation of DsRed-labeled *M. loti* (Maekawa *et al.*, 2009), infection events, including IT formation and nodule organogenesis, occurred on the roots of wt/*pEpi::GUS*$^+$ to an equivalent extent as the roots of wt/*p35S::GUS*$^+$. These observations indicate that heterologous gene expression via *pEpi* does not affect rhizobial infection processes (Table 1 and Figure S5).

Expression analysis of symbiotic genes in root hairs

In addition to the *LjEXPA* genes, we examined relative expression levels of several symbiotic genes in root hairs and stripped roots with or without *M. loti* inoculation. Two days after inoculation of *M. loti* or mock inoculation, all genes were found to be expressed in root hairs as well as in stripped roots. Among the genes examined, *NUP85* and *NSP2* showed a significant root hair expression pattern (Figure S6). Inoculation of *M. loti* caused increases in both *NSP1* and *NIN* expression in both root hairs and stripped roots (Figure S6). In contrast, the expression of other symbiotic genes remained unchanged after inoculation of *M. loti* (Figure S6).

pEpi::CCaMK induces the formation of ITs in epidermis, but infection events in the cortex do not occur

CCaMK is involved not only in rhizobial infection through ITs (Hayashi *et al.*, 2010) but also in nodule organogenesis in the cortex (Tirichine *et al.*, 2006). Spatio-temporal expression of *CCaMK*, analyzed by introduction of the GUS gene driven by the CCaMK promoter (*pCCaMK::GUS*), showed both epidermal and cortical expression in *Lotus* roots (Figure 2a–d). Based on the expression pattern of *CCaMK*, we examined whether the *Epi* promoter confers epidermis-specific expression of target genes in *L. japonicus* by complementation of the symbiotic phenotypes of the *ccamk–3* mutant using the *pEpi* expression system.

Table 1 Complementation analysis of symbiosis-defective phenotypes using the *pEpi* expression system

		Root hair phenotype (%)				Nodulation phenotype (%)				
Lotus line	Construct	No colonization	Micro-colony	Short ITs	ITs	Nod$^-$	Bump	Nod	Nodules per nodulated plant (mean ± SE)	Total number of plants
Wild-type	Empty	0	0	0	100	0	0	100	17.5 ± 1.1	31
Wild-type	*pEpi::GUS*$^+$	0	0	0	100	0	0	100	22.7 ± 1.8	35
Wild-type	*p35S::GUS*$^+$	0	0	0	100	0	0	100	20.9 ± 1.5	30
nfr1–4	Empty	100	0	0	0	100	0	0	–	20
nfr1–4	*pEpi::NFR1*	0.9	34.9	44.9	19.3	7.3	67.9	24.8	1.1 ± 0.1	109
nfr1–4	*p35S::NFR1*	0	0	0	100	0	0	100	18.3 ± 0.8	65
nfr5–2	Empty	100	0	0	0	100	0	0	–	51
nfr5–2	*pEpi::NFR5*	0	12.2	50	37.8	4.9	18.3	76.8	6.0 ± 0.6	82
nfr5–2	*p35S::NFR5*	0	0	0	100	0	0	100	13.5 ± 1.0	44
nup85–2	Empty	100	0	0	0	100	0	0	–	59
nup85–2	*pEpi::NUP85*	0	0	0	100	0	0	100	15.3 ± 0.6	102
nup85–2	*p35S::NUP85*	0	0	0	100	0	0	100	18.0 ± 0.8	93
nup133–3	Empty	100	0	0	0	100	0	0	–	67
nup133–3	*pEpi::NUP133*	0	0	0	100	2.3	0	97.7	9.8 ± 0.6	87
nup133–3	*p35S::NUP133*	0	0	0	100	0	0	100	11.2 ± 0.7	60
castor–4	Empty	100	0	0	0	100	0	0	–	21
castor–4	*pEpi::CASTOR*	0	0	0	100	0	0	100	23.0 ± 1.8	54
castor–4	*p35S::CASTOR*	0	0	0	100	0	0	100	19.4 ± 1.2	48
pollux–3	Empty	100	0	0	0	100	0	0	–	50
pollux–3	*pEpi::POLLUX*	0	0	0	100	0	0	100	20.5 ± 1.3	55
pollux–3	*p35S::POLLUX*	0	0	0	100	0	0	100	18.7 ± 1.3	64
ccamk–3	Empty	100	0	0	0	100	0	0	–	88
ccamk–3	*pEpi::CCaMK*	0	3.7	0.9	95.4	58.3	13.9	27.8	2.2 ± 0.4	108
ccamk–3	*p35S::CCaMK*	0	0	0	100	0	0	100	11.5 ± 0.9	55
cyclops–3	Empty	0	86.1	13.9	0	0	100	0	–	36
cyclops–3	*pEpi::CYCLOPS*	0	0	0	100	0	100	0	–	90
cyclops–3	*p35S::CYCLOPS*	0	0	0	100	0	0	100	12.5 ± 1.0	78
nsp1–1	Empty	100	0	0	0	100	0	0	–	61
nsp1–1	*pEpi::NSP1*	0	0	0	100	58.1	17.7	24.2	1.7 ± 0.4	62
nsp1–1	*p35S::NSP1*	0	0	0	100	0	0	100	16.1 ± 1.0	67
nsp2–1	Empty	100	0	0	0	100	0	0	–	61
nsp2–1	*pEpi::NSP2*	5.3	11.6	8.4	74.7	96.8	2.1	1.1	1.0	95
nsp2–1	*p35S::NSP2*	0	0	0	100	0	0	100	16.4 ± 1.9	39

The numbers indicate the percentage of plants that showed infection events, i.e. formation of micro-colonies or infection threads (ITs) in the epidermis, and nodulation events, i.e. formation of empty nodules (bump) or infected nodules (Nod) in the cortex, 4 weeks after inoculation of DsRed-labeled *Mesorhizobium loti*. Data were compiled from more than two independent experiments. Wild-type, Gifu B–129; Empty, empty vector; *pEpi*, Epi308 promoter; *p35S*, CaMV 35S promoter.

Neither IT formation nor nodule formation was induced on *ccamk* roots transformed with the empty vector control upon *M. loti* inoculation (Figure S7), or on any symbiotic mutant examined in this study (Figures S7 and S8). In contrast, the roots of *ccamk*/*p35S::CCaMK* plants formed nodules associated with the development of ITs from curled root hairs to the cortex (Figure 2h–j). Introduction of *pEpi::CCaMK* resulted in rescue of epidermal infection events, including root hair curling and well-developed ITs within root hairs, while penetration of ITs into the cortical cell layer was rarely observed (Figure 2e–g).

To evaluate the effectiveness of the *pEpi* expression system more thoroughly, the number of nodules per nodulated plant and the frequency distribution of cortical cell division were investigated 4 weeks after inoculation (Table 1 and Figure S9). Mature nodules and nodule primordia in which infected cells are visualized with red fluorescence (derived from DsRed-labeled *M. loti*) are defined as 'nodules'. In contrast, empty nodule-like structures, in which red fluorescence was not observed, are defined as 'bumps'. In the case of *ccamk*/*p35S::CCaMK*, all plants formed nodules (indicated by red bars in Figure S9) and the mean number of nodules per nodulated plant was 11.5 ± 0.9 (Table 1). On the roots of *ccamk*/*pEpi::CCaMK*, over 50% of the plants showed a non-nodulation phenotype (Nod$^-$, indicated by black bars in Figure S9). Although cortical cell division was induced, the number of nodules per nodulated plant was lower (2.2 ± 0.4; Table 1) than that of *ccamk*/*p35S::CCaMK*. These data demonstrate that expression of *CCaMK* via the *pEpi* expression system is

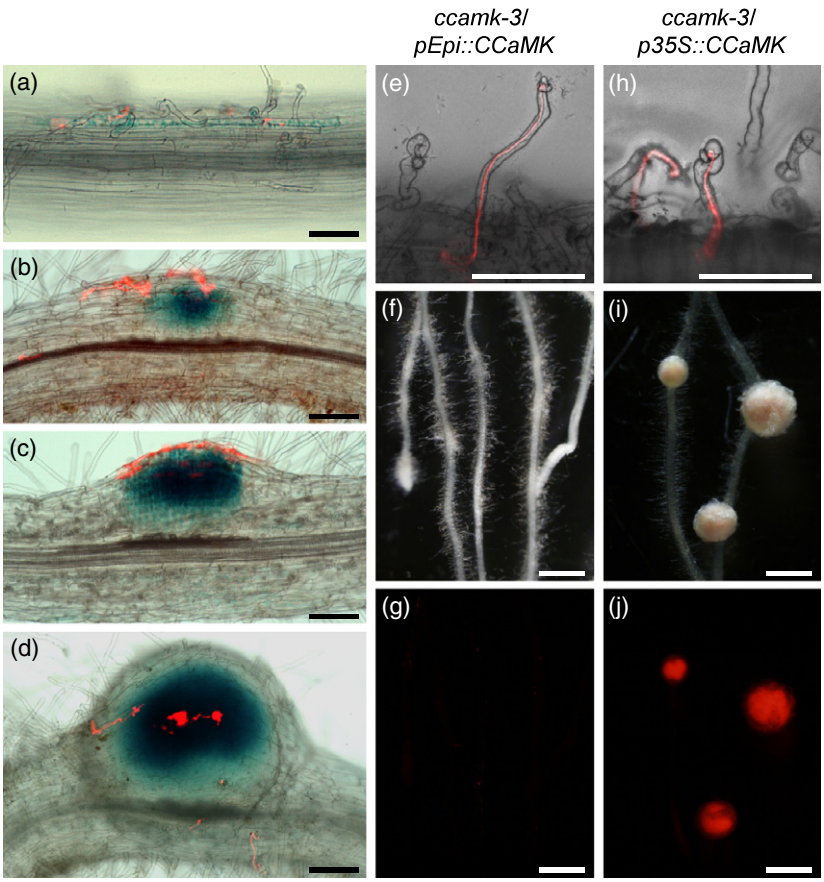

Figure 2. Histochemical localization of GUS activity in wild-type roots transformed with *pCCaMK::GUS* vector, and complementation tests of rhizobial infection and nodule organogenesis phenotypes of the *ccamk–3* mutant transformed with *CCaMK* driven by *pEpi* or *p35S*.
(a–d) GUS expression patterns for wild-type roots transformed with *pCCaMK::GUS* vector after inoculation with DsRed-labeled *Mesorhizobium loti*. Bright-field and red fluorescence images were merged into single images. (a) Root hairs of wt/*pCCaMK::GUS* roots observed 7 days after inoculation with *M. loti*. (b–d) Development of nodules on the wt/*pCCaMK::GUS* roots 10 days after inoculation with *M. loti*. Blue staining was observed in curled root hairs (a), in cortical cells before cortical infection thread (IT) formation (b), and during cortical cell division (c) and cortical infection (d).
(e–j) Symbiotic phenotypes of transformed roots were observed 4 weeks after inoculation with DsRed-labeled *M. loti*. (e, h) Root hairs of *ccamk–3*/*pEpi::CCaMK* and *ccamk–3*/*p35S::CCaMK*, shown as merged bright-field and red fluorescence images. ITs are visible inside the curled root hairs. Bright-field images (f, i) and corresponding red fluorescence images (g, j) for nodulation phenotypes are shown. (i) Nodules formed on the roots of *ccamk–3*/*p35S::CCaMK* plants. (j) Infection of DsRed-labeled *M. loti* was observed as red fluorescence in the central zone of nodules. (f, g) Nodule organogenesis was not induced on the roots of *ccamk–3*/*pEpi::CCaMK*. Scale bars = 100 μm (a–e, h) and 1 mm (f, g, i, j).

sufficient for epidermal IT formation, but is not sufficient to induce cortical IT formation or cortical cell division. These phenotypes are in agreement with the report by Rival *et al.* (2012), in which epidermal expression of *DMI3* genes via the LeEXT promoter rescues only the epidermal infection phenotype of the *dmi3* mutant of *M. truncatula*.

As previously reported (Hayashi *et al.*, 2010), introduction of the gain-of-function gene *CCaMK*^{T265D} under the control of the CaMV 35S promoter (*p35S*) induced spontaneous nodulation in the absence of rhizobia (Figure S10). To examine whether epidermal expression of CCaMK^{T265D} induces spontaneous nodulation, *pEpi::CCaMK*^{T265D} was introduced into wild-type roots. Spontaneous nodulation was not observed on the roots of wt/*pEpi::CCaMK*^{T265D} or those of wt/*pEpi::CCaMK*^{T265T} even 6 weeks after transplantation (Figure S10 and Table S1). These results suggest that expression of *CCaMK*^{T265D} in the cortex is indispensable for spontaneous nodule formation.

Taking these results together, the *pEpi* expression system can be regarded as an epidermis-specific expression system in *Lotus* roots, based on the phenotypes observed on the roots of both *ccamk*/*pEpi::CCaMK* and wt/*pEpi::CCaMK*^{T265D}. Furthermore, the *pEpi* expression system shows that there is a requirement for cortical CCaMK expression in cortical IT formation and nodule organogenesis.

Expression of upstream genes in the epidermis is sufficient for both epidermal and cortical infection events

The *nup85*, *nup133*, *castor* and *pollux* mutants transformed with their corresponding genes driven by *p35S* formed nodules upon *M. loti* inoculation (Table 1 and

Figure S11), while *symrk*/*p35S::SYMRK* did not form effective nodules. Accordingly, we examined the function of *NUP85*, *NUP133*, *CASTOR* and *POLLUX* by the *pEpi* expression system. Expression of these genes driven by *pEpi* rescued the symbiotic defects in their corresponding mutants, resulting in the formation of nodules (Table 1 and Figure 3). A sequence of infection events, including root hair curling, IT development from epidermis to cortex and the formation of nodules, were observed, comparable to those in mutants transformed with *p35S* to drive the corresponding genes (Table 1, Figures 3 and S11). These results indicate that expression of upstream genes in the epidermis is sufficient for both rhizobial infection and nodule organogenesis.

Dispensability of Ca^{2+} signal-responsive domains of CCaMK for cortical infection processes

Expression of upstream genes by the *pEpi* expression system is sufficient to induce the complete nodulation process. In contrast, the complementation results for both *ccamk*/*pEpi::CCaMK* and wt/*pEpi::CCaMK*^{T265D} suggest that there is a requirement for cortical CCaMK expression for cortical IT formation and nodule organogenesis. Upstream genes encode the components of machinery for Ca^{2+} spiking, which is believed to be an activator for CCaMK (Singh and Parniske, 2012). Therefore, our results raise questions about whether CCaMK activation by cortical Ca^{2+} spiking via upstream components is essential for cortical infection processes. CCaMK contains a calmodulin-binding domain (CaMBD) and Ca^{2+}-binding EF hands at its C–terminus. The CaMBD and EF hands respond to Ca^{2+} signals and act as regulatory domains for CCaMK. Among the C–terminus-deleted CCaMKs examined in our previous work, CCaMK1–314 (lacking CaMBD and EF hands) and CCaMK1–340 (lacking EF hands) lost the ability to bind calmodulin and Ca^{2+} *in vitro* (Shimoda *et al.*, 2012). Complementation analysis of the *ccamk* mutant by the truncated CCaMKs showed a loss of function of both CCaMKs for rhizobial infection, demonstrating that CaMBD and EF hands play an essential role in IT formation. In contrast to CCaMK1–340, which also showed a loss of function for nodule organogenesis, CCaMK1–314 showed a gain of function for nodule organogenesis, in the sense that spontaneous nodulation was induced on the roots of *ccamk*/*p35S::CCaMK1–314* (Shimoda *et al.*, 2012).

To evaluate the requirement of the C–terminus regulatory domains of CCaMK for cortical infection processes, we developed a simultaneous expression system comprising two target genes expressed under the control of two distinct promoters, *p35S* and *pEpi* (Figure 4). Under the control of *p35S*, the first target gene is expressed in whole roots including the epidermis and cortex, while *pEpi* allows expression of the second target gene only in the epidermis. Using the *pEpi*+*p35S* double expression system, we

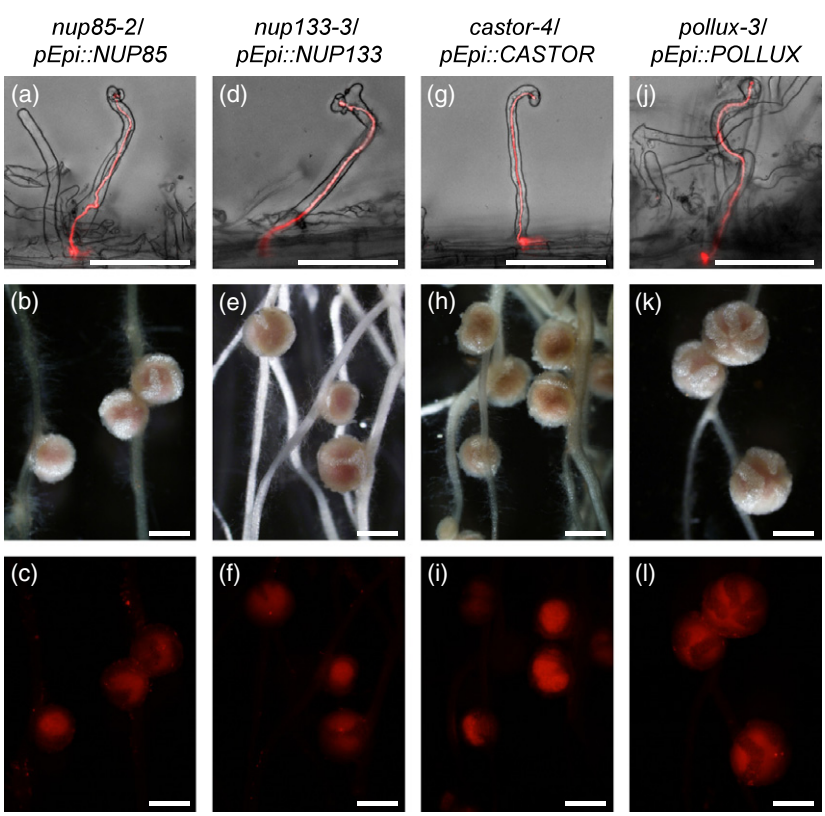

Figure 3. Complementation tests of rhizobial infection and nodule organogenesis phenotypes of *nup85–2*, *nup133–3*, *castor–4* and *pollux–3* mutants transformed with the corresponding genes driven by *pEpi*.
Symbiotic phenotypes of transformed roots were observed 4 weeks after inoculation with DsRed-labeled *Mesorhizobium loti*. Root phenotypes of *nup85–2*/*pEpi::NUP85* (a–c), *nup133–3*/*pEpi::NUP133* (d–f), *castor–4*/*pEpi::CASTOR* (g–i) and *pollux–3*/*pEpi::POLLUX* (j–l). (a, d, g, j) ITs are visible inside the curled root hairs, shown as merged bright-field and red fluorescence images. Bright-field images (b, e, h, k) and corresponding red fluorescence images (c, f, i, l) for nodulation phenotypes are shown. (c, f, i, l) Infection of DsRed-labeled *M. loti* was observed as red fluorescence in the central zone of nodules. Scale bars = 100 μm (a, d, g, j) and 1 mm (b, c, e, f, h, i, k, l).

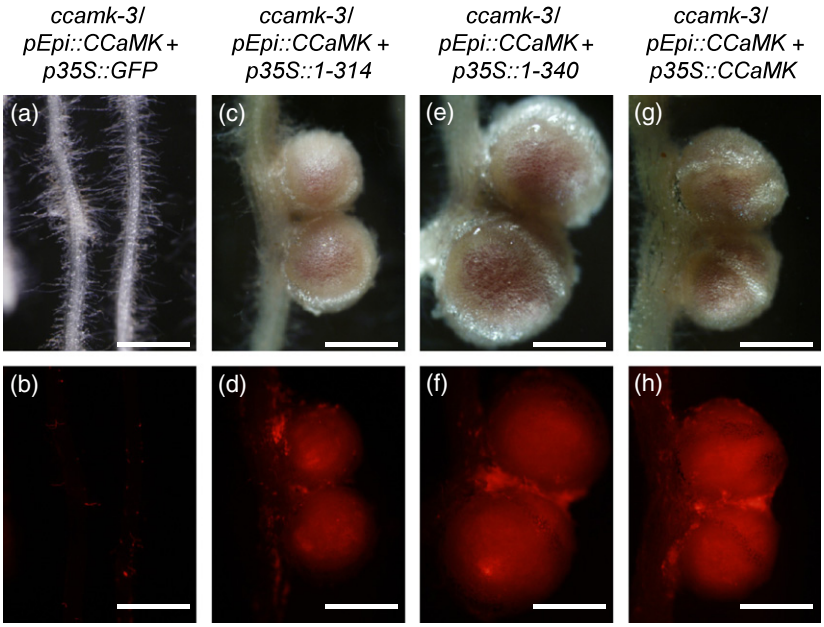

Figure 4. Complementation tests of nodulation phenotypes of the *ccamk–3* mutant by co-transformation with *CCaMK* under the control of *pEpi* and truncated *CCaMK1–314* or *CCaMK1–340* under the control of *p35S*.
Nodulation phenotypes of transformed roots were observed 4 weeks after inoculation with DsRed-labeled *Mesorhizobium loti*. Bright-field images (a, c, e, g) and their corresponding red fluorescence images (b, d, f, h) for nodulation phenotypes are shown. Nodule organogenesis was not induced on the roots of *ccamk–3/pEpi::CCaMK+p35S::GFP* (a, b). Nodules formed on the roots of *ccamk–3/pEpi::CCaMK+p35S::CCaMK1–314* (c, d), *ccamk–3/pEpi::CCaMK+p35S::CCaMK1–340* (e, f) and *ccamk–3/pEpi::CCaMK+p35S::CCaMK* (g, h). Infection of DsRed-labeled *M. loti* was observed as red fluorescence in the central zone of nodules (d, f, h). Scale bars = 1 mm.

Table 2 Complementation analysis of symbiosis-defective phenotypes using the *pEpi+p35S* double expression system

		Nodulation phenotype (%)					
Lotus line	Construct	Nod$^-$	Bump	Nod	Nodules per nodulated plant (mean ± SE)	Spontaneous nodule-like structures per nodulated plant (mean ± SE)	Total number of plants
ccamk–3	*pEpi::CCaMK+p35S::GFP*	46.3	11.9	41.8	2.5 ± 0.3	–	67
ccamk–3	*pEpi::CCaMK+p35S::CCaMK1–314*	9.8	9.8	80.4	5.2 ± 0.4	0.7 ± 0.1	92
ccamk–3	*pEpi::CCaMK+p35S::CCaMK1–340*	15.7	1.2	83.1	7.6 ± 0.6	–	83
ccamk–3	*pEpi::CCaMK+p35S::CCaMK*	3.3	0	96.7	9.6 ± 0.7	–	91

The numbers indicate the percentage of plants that showed nodulation events, i.e. formation of empty nodules (bump) or infected nodules (Nod) in the cortex, 4 weeks after inoculation of DsRed-labeled *Mesorhizobium loti*. Data were compiled from more than two independent experiments. *pEpi*, Epi308 promoter; *p35S*, CaMV 35S promoter.

introduced *pEpi::CCaMK+p35S::CCaMK1–314* into *ccamk* roots. Following the formation of epidermal ITs, cortical ITs associated with cortical cell division occurred, resulting in the formation of nodules (Table 2, Figures 4 and S12). Similar phenotypes were also observed on the roots of *ccamk/pEpi::CCaMK+p35S::CCaMK1–340*. In the case of *pEpi::CCaMK+p35S::CCaMK1–314*, spontaneous nodule-like structures were occasionally formed (Table 2 and Figure S13). This phenotype is considered to be an indication of a gain of function of CCaMK1-314 for nodule organogenesis. These results show not only an absolute requirement of full-length CCaMK for epidermal IT formation, but dispensability of the Ca^{2+}-responsive domains of CCaMK for cortical infection processes. Taking these results into account, our results suggest that activation of CCaMK via upstream genes in the epidermis is essential for the formation of epidermal ITs, but the symbiotic function of CCaMK in the cortex does not necessarily depend on Ca^{2+} and calmodulin.

CYCLOPS appears to be indispensable for IT formation in both the epidermis and cortex

On the roots of *cyclops* mutants, IT development accompanied by rhizobial infection is arrested in the epidermis, resulting in the formation of small bumps without infected cells (Figure S14). *pEpi::CYCLOPS* restored epidermal infection defects in the *cyclops* mutant, as did *p35S::CYCLOPS* (Table 1 and Figure S14), but cortical IT development was not rescued, resulting in the formation of bumps (Table 1, Figures S14 and S15). These results show that *CYCLOPS* expression under the control of *pEpi* is insufficient for cortical IT development, suggesting that cortical expression of *CYCLOPS* is indispensable for bacterial entry into the cortex.

Epidermal expression of *NSP1* and *NSP2* only restores epidermal IT formation on the roots of the corresponding mutants

On the roots of both *nsp1*/*pEpi::NSP1* and *nsp2*/*pEpi::NSP2*, micro-colony and IT formation in the epidermis were restored (Table 1 and Figure S16). However, neither cortical cell division nor IT development into the cortex occurred on these roots. The majority of the plants showed a non-nodulation phenotype (Figure S15), and the number of nodules per nodulated plant was lower than those of *nsp1*/*p35S::NSP1* and *nsp2*/*p35S::NSP2* plants (Table 1 and Figure S15). Taken together, *NSP1* and *NSP2* appear to be indispensable not only for IT formation in the epidermis, but also for IT development and nodule organogenesis in the root cortex.

Different requirements of NFR1 and NFR5 expression for IT development

NFR1 and NFR5, LysM-like receptor kinases that bind to Nod factors derived from *M. loti*, are considered to be the starting point of root nodule symbiosis in *Lotus* (Broghammer *et al.*, 2012). Their corresponding mutants are deficient in any symbiotic responses, including deformation of root hairs and the formation of ITs (Radutoiu *et al.*, 2003). Introduction of both genes into the corresponding mutants via the *pEpi* expression system led to the deformation of root hairs, the colonization of bacteria in curled root hairs, and the formation of ITs within root hairs (Table 1 and Figure 5a,d). However, the frequency of epidermal ITs (19.3% on the roots of *nfr1*/*pEpi::NFR1*; 37.8% on the roots of *nfr5*/*pEpi::NFR5*) were lower than those on *nfr1*/*p35S::NFR1* or *nfr5*/*p35S::NFR5* (100%; Table1 and Figure 5g,j).

In the cortex of *nfr1*/*pEpi::NFR1* roots, although cortical cell division was induced, almost all of nodule primordia were arrested at bumps, and nodules were rarely formed (Table 1, Figures 5b,c and S15). In contrast, the majority of cortical cell division resulted in formation of nodules on the roots of *nfr5*/*pEpi::NFR5*, while the number of nodules per nodulated plant was lower than that on *nfr5*/*p35S::NFR5* (Table 1, Figures 5e,f,k,l and S15). These results suggest that expression of *NFR1* and *NFR5* in root epidermis is sufficient for the induction of cortical cell division, but the involvement of NFR1 and NFR5 for cortical IT formation appears to be different from each other.

DISCUSSION

Construction and evaluation of the *pEpi* expression system in *Lotus japonicus*

We have previously reported epistatic relationships among symbiotic genes in both IT formation and nodule organogenesis (Hayashi *et al.*, 2010). However, the individual requirements of symbiotic genes for cell-layer events

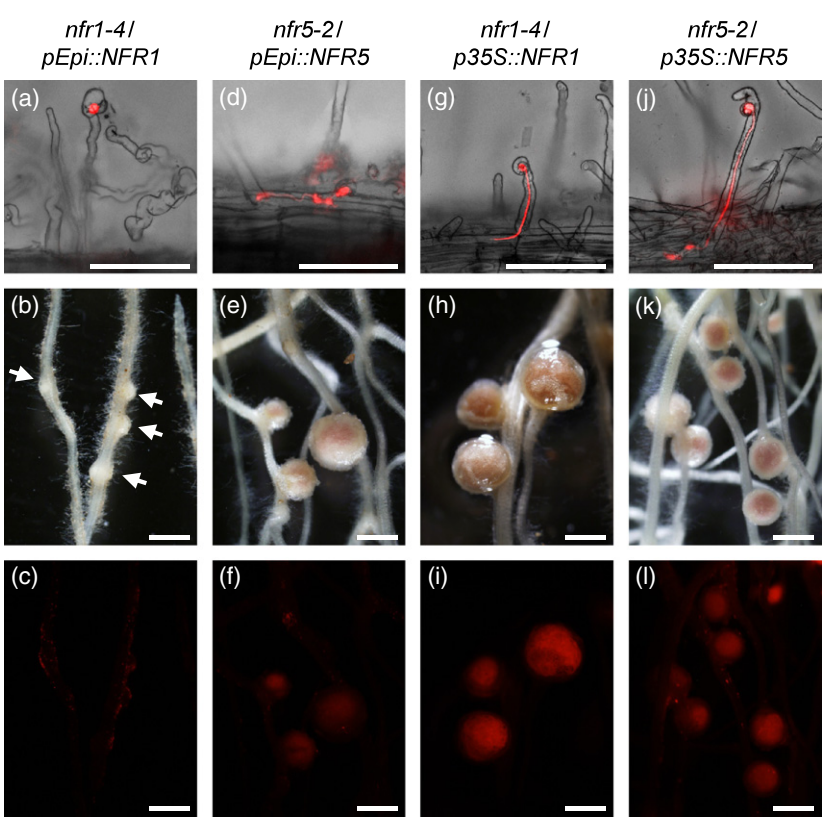

Figure 5. Complementation tests of rhizobial infection and nodule organogenesis phenotypes of *nfr1–4* and *nfr5–2* mutants transformed with the corresponding genes driven by *pEpi* or *p35S*.
Symbiotic phenotypes of transformed roots were observed 4 weeks after inoculation with DsRed-labeled *Mesorhizobium loti*. Root hairs of *nfr1–4*/*pEpi::NFR1* (a), *nfr5–2*/*pEpi::NFR5* (d), *nfr1–4*/*p35S::NFR1* (g) and *nfr5–2*/*p35S::NFR5* (j) are shown as merged images of bright-field and red fluorescence images. (a) Although deformation of root hairs and colonization of bacteria in curled root hairs occurred, development of ITs within root hairs rarely occurred on the roots of *nfr1–4*/*pEpi::NFR1*. (d, g, j) ITs are visible inside the curled root hairs of *nfr5–2*/*pEpi::NFR5* (d), *nfr1–4*/*p35S::NFR1* (g) and *nfr5–2*/*p35S::NFR5* (j). Bright-field images (b, e, h, k) and their corresponding red fluorescence images (c, f, i, l) of nodulation phenotypes are shown. (b, c) Almost 70% of cortical cell division was arrested, resulting in bump structures (arrows), and effective nodules rarely formed on the roots of *nfr1–4*/*pEpi::NFR1*. Nodules formed on the roots of *nfr5–2*/*pEpi::NFR5* (e), *nfr1–4*/*p35S::NFR1* (h) and *nfr5–2*/*p35S::NFR5* (k). (f, i, l) Infection of DsRed-labeled *Mesorhizobium loti* was observed as red fluorescence in the central zone of nodules. Scale bars = 100 μm (a, d, g, j) and 1 mm (b, c, e, f, h, i, k, l).

including epidermal IT formation, cortical IT formation and cortical cell division remain unclear. In this study, we developed a '*pEpi* expression system' using the promoter regions of two *Lotus expansin* genes, *LjEXPA7* and *LjEXPA8*. As reported for *AtEXPA7* and orthologous genes of angiosperm species (Kim *et al.*, 2006), the promoter regions of both *LjEXPA7* and *LjEXPA8* contain conserved RHEs. Detailed evaluation of our *pEpi* expression system was performed based on: (i) gene expression analysis of root hairs and stripped roots of *Lotus* by quantitative RT–PCR, and (ii) spatio-expression analysis of *pEpi::GUS*$^{+}$ constructs. Among the candidates examined, we selected *pEpi308*, a promoter region of *LjEXPA7* containing three RHE motifs (Figure 1), and developed the *pEpi* expression system. Subsequently, we examined the symbiotic phenotypes of *ccamk* mutants transformed with CCaMK and CCaMK^{T265D} using the *pEpi* expression system. The roots of *ccamk*/*pEpi::CCaMK* showed IT formation in the epidermis, but IT development into the cortex and cortical cell division were not recovered (Figure 2e–g). Moreover, no spontaneous nodules were formed on the roots of *ccamk*/*pEpi::CCaMK*^{T265D} (Figure S10). Collectively, these data show the utility of the *pEpi* expression system to analyze the effects of epidermal expression of other symbiotic genes on epidermal and cortical infection processes.

Cell layer-specific differences in requirements for upstream gene expression during nodulation

Epidermal expression of upstream genes, including *NUP85*, *NUP133*, *CASTOR* and *POLLUX*, by the *pEpi* expression system, perfectly rescued all of the symbiotic defects in the corresponding gene mutants, leading to formation of nodules (Table 1, Figures 3 and S9). There is the possibility of leakage of gene products from epidermis to cortex, but, in the case of upstream genes, almost all cortical cell division resulted in the formation of nodules, as shown in Figure S9. These clear-cut complementation results were restricted to the upstream genes examined (Figures 3 and S9), and were not observed for *CCaMK*, *CYCLOPS*, *NSP1* and *NSP2* (Figures 2 and S9, S14, S15 and S16). On the basis of these results, we suggest that, once the epidermal infection process is completed, cortical infection processes no longer require expression of the upstream components in the cortex (Figure 6).

The upstream genes are responsible for the induction of Ca^{2+} spiking, which acts as a second messenger activating the downstream symbiotic pathway. Actually, almost all symbiotic mutants of upstream genes showed a non-nodulation phenotype. In the case of *L. japonicus*, two of the upstream gene mutants, *nena–1* and *symrk–14*, also did not induce Ca^{2+} spiking and showed impaired ability to develop epidermal ITs. However, cortical IT formation and nodule organogenesis occurred normally, leading to the formation of nodules (Groth *et al.*, 2010; Kosuta *et al.*, 2011). In both cases, rhizobia invaded the host plants via intercellular 'crack entry' rather than through intracellular epidermal ITs. These phenotypes are in line with our proposed model in which the induction of Ca^{2+} spiking is required for epidermal IT formation but is not required for cortical IT formation in *L. japonicus*.

Different requirements of Ca^{2+}-responsive regulatory domains of CCaMK for infection processes in *L. japonicus*

It is generally accepted that Ca^{2+}-dependent activation of CCaMK is essential for intracellular accommodation of rhizobia. Furthermore, we revealed the importance of CaMBD and EF hands of CCaMK for IT formation (Shimoda *et al.*, 2012). To evaluate the hypothesis that cortical infection processes do not require CCaMK activation by cortical Ca^{2+} spiking, we expressed Ca^{2+}-responsive domain-deleted CCaMKs under the control of *p35S*, concurrently with expression of full-length CCaMK under the control of *pEpi*, in a *ccamk* mutant. When accompanied by epidermal expression of full-length CCaMK, these domain-deleted

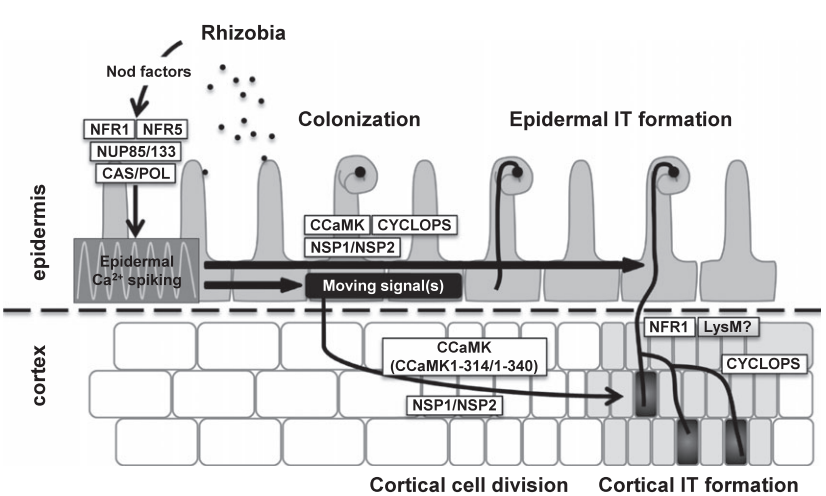

Figure 6. Model for coordinated infection processes regulated by symbiotic genes examined in this study. Ca^{2+} spiking, induced through NFR1/NFR5 and upstream genes, is indispensable for the development of epidermal ITs within root hairs. Downstream of the epidermal Ca^{2+} spiking, CCaMK, CYCLOPS and NSP1/NSP2 function to form epidermal ITs. The epidermal Ca^{2+} spiking is also involved in generation of unidentified 'moving signal(s)' that trigger cortical cell division. Once epidermal ITs form, Ca^{2+} spiking in the cortex is not necessarily required for development of cortical ITs. NFR1 and other LysM receptors may act together to perceive Nod factors, leading to invasion of rhizobia through cortical ITs. CAS, CASTOR; POL, POLLUX.

CCaMKs regulated cortical infection processes (Table 2 and Figure 4), strengthening the hypothesis that CCaMK activation by cortical Ca^{2+} spiking is not essential for cortical infection processes in *L. japonicus* (Figure 6).

In contrast to the reports in *L. japonicus*, an important role for cortical Ca^{2+} spiking for intracellular cortical infection has been reported in *M. truncatula*. Cortical Ca^{2+} spiking was triggered during initial stages of IT formation in the outer roots cortex, and was proposed to play an important role for the navigation of cortical IT development (Sieberer *et al.*, 2012). In this view, full-length DMI3 was thought to be required for both epidermal and cortical nodulation processes in *M. truncatula*. However, combined epidermal and cortical expression of full-length *DMI3* via two promoters, *pLeEXT* (epidermis) and *pCO2* (cortex), only complemented nodule organogenesis of the *dmi3* mutant, resulting in the formation of empty nodules (Rival *et al.*, 2012). The result for *dmi3*/*pLeEXT*+*pCO2::DMI3* raises the question of whether *pCO2* confers a sufficient level of gene expression in the cortex.

Medicago truncatula forms indeterminate nodules that retain a persistent nodule meristem. ITs grow and penetrate through the outer cortex towards the dividing inner cortex, which constitutes the nodule meristem, and the host plant cells continue to be infected by rhizobia during nodule development (Hirsch, 1992). In contrast, *L. japonicus* forms determinate nodules that lack a persistent nodule meristem. Following cortical cell division, which ceases early during nodule development, cell expansion accompanied by bacterial invasion through ITs occurs once. These differences between indeterminate and determinate nodulation have led to speculation that the importance of cortical Ca^{2+} spiking for IT formation in *M. truncatula* is different from that of *L. japonicus*. Further analyses of the requirement for cortical Ca^{2+} spiking and the functionality of CCaMK/DMI3 in cortex are necessary to provide missing pieces in our understanding of the importance of Ca^{2+}-mediated signal transduction for accommodation of rhizobial bacteria, and also provide information about the various mechanisms by which indeterminate and determinate nodulation are governed.

In *L. japonicus*, cell type-specific regulation of rhizobial infection by CCaMK was reported by Liao *et al.* (2012), based on the phenotypes of a *ccamk–14* mutant that showed excess epidermal IT formation in parallel with abnormal cortical IT formation. The *ccamk–14* mutation is caused by a S337N substitution in the CaMBD. The S337 residue is a target of autophosphorylation, and has been reported to be responsible for negative regulation of CCaMK via Ca^{2+}/calmodulin binding (Liao *et al.*, 2012). The S337N mutation prevents CCaMK from the negative feedback regulation that appears to be essential for cortical IT formation (Liao *et al.*, 2012). These phenotypes appear to be contradictory with our data; however, both CCaMK1–314 and CCaMK1–340 are considered to be kept in an inactive state and retain the ability to regulate cortical infection. Thus, the truncated CCaMKs may be regarded as potentially functional CCaMKs for the regulation of cortical IT formation.

Symbiotic genes responsible for cortical infection processes

In the case of *CYCLOPS*, although epidermal IT formation recovered, symbiosis-defective phenotypes, e.g. arrested development of cortical ITs and formation of bumps, were retained on the roots of *cyclops*/*pEpi::CYCLOPS*. As previously reported, CYCLOPS is not necessarily required for the induction of cortical cell division, as spontaneous nodulation occurs on the roots of *cyclops*/*p35S::CCaMK*^{T265D} (Yano *et al.*, 2008). Taken together, the results suggest that the loss of complementation of cortical infection defects on the roots of *cyclops*/*pEpi::CYCLOPS* is due to incomplete development of cortical ITs (Figure 6), indicating a requirement of CYCLOPS for both epidermal and cortical IT formation.

Similarly to *CCaMK*, expression of *NSP1* and *NSP2* by *pEpi* did not complement cortical infection events of *nsp1* and *nsp2* mutants, respectively. Collectively, these results indicate that *NSP1* and *NSP2* are indispensable for cortical IT formation and cortical cell division (Figure 6).

Different involvement of NFR1 and NFR5 in rhizobial infection processes

Each of the symbiotic genes expressed via the *pEpi* expression system rescued the epidermal responses in the corresponding gene mutants, except for *NFR1* and *NFR5* (Table 1, Figures 5 and S15). Root hair curling occurred on the roots of both *nfr1*/*pEpi::NFR1* and *nfr5*/*pEpi::NFR5*, but development of ITs within root hairs occurred at a very low frequency compared with the other mutants examined (Table 1). These results suggest that the transcript level of both *NFR1* and *NFR5* under the control of *pEpi* may be insufficient for the entire process of IT development in the epidermis.

In this study, the *pEpi* expression system was used to elucidated the distinct requirements of *NFR1* and *NFR5* for cortical infection processes in *L. japonicus*. On the roots of *nfr5*/*pEpi::NFR5*, the majority of nodule primordia resulted in the formation of nodules, although the number of nodules per nodulated plant was lower than that of *nfr5*/*p35S::NFR5* plants (Table 1, Figures 5 and S15). In contrast, almost 70% of cortical cell division was arrested at bumps, and nodules were rarely formed on the roots of *nfr1*/*pEpi::NFR1* (Table 1, Figures 5b,c and S15).

In general, rhizobia are thought to produce Nod factors continuously within developing ITs (Timmers *et al.*, 1998). Taking this into account, our results suggest that Nod factor signaling through NFR1/NFR5 is crucial for the

development of ITs in the epidermis. Complementation defects of *nfr1*/*pEpi::NFR1* in cortical IT formation also imply the requirement of NFR1 for perception and signaling of Nod factors throughout IT development. Compared to NFR1, the involvement of NFR5 for cortical IT development is somewhat attenuated, suggesting the possibility that NFR1 may form a receptor complex with LysM receptor homologs other than NFR5 (Figure 6; Arrighi *et al.*, 2006; Lohmann *et al.*, 2010), with which NFR1 perceives Nod factors and regulates cortical IT formation. In contrast to *NFR5* in *Lotus*, *NFP*, an ortholog of *NFR5* in *M. truncatula*, did not complement cortical IT formation on the roots of *nfp*/*pLeEXT::NFP* (Rival *et al.*, 2012). In the case of *M. truncatula*, *LYK3*, an ortholog of *NFR1*, is not involved in the induction of Ca^{2+} spiking, and an *NFR1* homolog, that may be responsible for the induction of Ca^{2+} spiking, has not been identified. Further analyses of LysM receptor kinases are required to broaden our understanding how epidermal and cortical infection events are coordinated by multiple LysM receptors in *L. japonicus* and *M. truncatula*.

Generation of 'moving signal(s)' responsible for the induction of cortical cell division

Upon inoculation with *M. loti*, both *nfr1*/*pEpi::NFR1* and *nfr5*/*pEpi::NFR5* roots showed the induction of nodule organogenesis (Table 1 and Figure 5), suggesting that the perception of Nod factors through NFR1/NFR5 in the epidermis stimulates signal(s) that are transmitted from the epidermis to cortex, leading to the induction of nodule organogenesis (Figure 6).

Cytokinins are possible candidates for a 'moving signal' from epidermis to cortex (Oldroyd and Downie, 2008; Heckmann *et al.*, 2011). The essential role of cytokinins in nodulation has been demonstrated by genetic studies in *L. japonicus* and *M. truncatula* (Gonzalez-Rizzo *et al.*, 2006; Murray *et al.*, 2007; Tirichine *et al.*, 2007). Activation of a putative cytokinin receptor, *Lotus* histidine kinase (LHK1), has been suggested to be necessary for nodule organogenesis, as a gain-of-function mutation in *LHK1* (*snf2*) induces spontaneous nodulation in the absence of rhizobia (Tirichine *et al.*, 2007). Using the cytokinin-responsive *ARR5* gene promoter fused to the GUS reporter gene, an increase of cytokinin levels was observed in curled and deformed root hairs and in dividing cortical cells after inoculation with *M. loti* (Lohar *et al.*, 2004). These results suggest that LHK1 in cortical cells acts as a receptor for cytokinins that may be transported from the epidermis, and that the activation of LHK1 induces subsequent steps of signaling pathways for nodule organogenesis.

GRAS domain proteins have been suggested to have the ability to move between cells, and their intercellular movement plays an important role for plant development (Cui *et al.*, 2007). Thus, NSP1 and NSP2 are also candidates for 'moving signals' from the epidermis to the cortex. We showed that neither *nsp1*/*pEpi::NSP1* nor *nsp2*/*pEpi::NSP2* roots induced nodule organogenesis upon inoculation with *M. loti*. Thus, movement of NSP1 or NSP2 from the epidermis to the cortex is considered not to be involved in the induction of nodule organogenesis, although we cannot rule out the possibility that the transcript levels of *NSP1* and *NSP2* driven by *pEpi* are quantitatively insufficient to allow intercellular movement and/or functioning of NSP1 and NSP2 in the cortex.

Expression analysis of symbiotic genes in root hairs

To isolate root hairs with high viability, samples of root hairs, stripped roots and whole roots were collected 2 days after inoculation of *M. loti* or mock inoculation. *LjEXPA7*, *LjEXPA8*, *LjRH101* and *LjRH102* transcripts were expressed at very high levels in isolated root hairs in comparison with stripped roots (Figures 1 and S2), indicating that enrichment of root hairs was successful. Expression analysis of symbiotic genes in root hairs and stripped roots showed that almost all symbiotic genes examined in this study are expressed in both regions (Figure S6). The root hair is a tubular outgrowth of the epidermis, thus stripped roots also contain some epidermal cells. Hence, it appears that comparison of root hairs with stripped roots is not sufficient to dissect epidermis-specific from cortex-specific expression of the symbiotic genes.

Importance of epidermal Ca^{2+} spiking for intracellular infection in *L. japonicus*

In this study, we did not directly analyze epidermal and cortical Ca^{2+} spiking during infection processes. However, the *pEpi* expression system provides evidence for cell layer-specific differences in the importance of Ca^{2+} spiking for IT formation. Intercellular infection via crack-entry overcame the requirement for Ca^{2+} spiking; however, the efficiency of intercellular infection is reduced in *L. japonicus* (Groth *et al.*, 2010; Madsen *et al.*, 2010; Kosuta *et al.*, 2011). These reports indicated the importance of Ca^{2+} spiking for establishment of intracellular infection via epidermis ITs as an effective infection route. Based on the strict recognition through Nod factor perception by LysM receptor kinases, Ca^{2+} spiking elicited in the epidermis appears to 'open the gate' for rhizobia by formation of ITs from the epidermis to the cortex.

EXPERIMENTAL PROCEDURES

Plant materials

Lotus japonicus B–129 accession Gifu (wild-type) and the mutants *nfr1–4* (Sandal *et al.*, 2006), *nfr5–2* (Madsen *et al.*, 2003), *castor–4* and *pollux–3* (Imaizumi-Anraku *et al.*, 2005), *nup85–2* (Saito *et al.*, 2007), *nup133–3* (Kanamori *et al.*, 2006), *ccamk–3* (Tirichine *et al.*, 2006), *cyclops–3* (Yano *et al.*, 2008), *nsp1–1* (Heckmann *et al.*, 2006) and *nsp2–1* (Murakami *et al.*, 2006) were used in this study. To visualize the infection processes of rhizo-

bia, *M. loti* MAFF303099 constitutively expressing DsRed (Maekawa *et al.*, 2009) was used.

Plasmid construction

Detailed information on plasmid construction is provided in Methods S1 and Table S2.

Hairy root transformation and inoculation tests with rhizobial strains

Induction and transformation of *L. japonicus* hairy roots using *A. rhizogenes* LBA1334 were performed as described by Díaz *et al.* (2005) with minor modifications. Plants with GFP-positive transformed hairy roots were selected by GFP fluorescence using a Leica MZFLIII stereomicroscope (Leica, http://www.leica-microsystems.com/) or an Olympus SZX12 stereomicroscope (Olympus, http://www.olympus-global.com/en/). The transformants were transplanted into vermiculite-containing pots supplied with half-strength B&D medium (Broughton and Dilworth, 1971) supplemented with 0.5 μM ammonium nitrate. Three days after transplantation, DsRed-labeled *M. loti* was inoculated onto the hairy roots of *L. japonicus*. The plants were grown in a growth cabinet under a 16 h day per 8 h night cycle at 24°C. Four weeks after inoculation, symbiotic phenotypes of plants with GFP-positive hairy roots were analyzed using an Olympus SZX12 stereomicroscope. In the case of the *pEpi::CCaMK+p35S* double expression system, hairy roots with epidermal ITs were selected as transformants and their phenotypes were analyzed, because the *pEpi::CCaMK+p35S* double expression system did not encode the GFP gene as a fluorescence marker.

GUS staining

The transformed roots were stained using 0.5 mg ml^{-1} 5–bromo-4–chloro-3–indolyl β–D–glucuronic acid cyclohexylammonium salt, 2.5 mM potassium ferricyanide, 2.5 mM potassium ferrocyanide and 10 mM EDTA in 100 mM sodium phosphate (pH 7.0), and incubated at 37°C in the dark. Samples were observed by using an Olympus SZX12 stereomicroscope or a light microscope (BZ–9000; Keyence, http://www.keyence.com/). For cross-sections, the stained roots were embedded in 5% agar and sectioned (50 μm thick) using a microslicer before observation.

Histological examination of rhizobial infection phenotypes

To examine the extent of rhizobial infection and nodule organogenesis, DsRed-expressing *M. loti* was observed using an Olympus SZX12 stereomicroscope equipped with a DP70 digital camera (Olympus). For observation of ITs, samples were analyzed under a BZ–9000 epifluorescence microscope (Keyence) using a filter set (excitation 560–600 nm band pass, emission 630–690 nm band pass). A Z–stack image was obtained using the BZ–9000 epifluorescence microscope with a step size of 2.5 μm (20 × objective) or 5 μm (10 × objective), and ten images of each stack were projected ('full-focused') onto a single plane to give an overall view of the samples using image processing software programs supplied with the BZ–9000 microscope.

RNA isolation from root hairs and real-time RT–PCR

The isolation of root hairs was performed as described by Maekawa *et al.* (2005) with some modifications. More detailed information, including the RNA extraction procedure, is provided in Methods S2. Reverse transcription was performed using a QuantiTect reverse transcription kit (Qiagen, http://www.qiagen.com/), followed by real-time quantitative PCR using LightCycler FastStart DNA Master^{PLUS} SYBR Green I (Roche, http://www.roche.com) in a Light Cycler system (Roche). *Lotus japonicus* ubiquitin (Flemetakis *et al.*, 2000) was used as the standard. *LjRH101* and *LjRH102*, which are expressed abundantly in the root hairs of *L. japonicus* (Maekawa *et al.*, 2005), were used as markers for biological identification of root hairs. All primers used for PCR are listed in Table S3.

ACKNOWLEDGEMENTS

We are grateful to Robert Ridge (Department of Life Science, International Christian University, Mitaka, Tokyo, Japan) for English editing of this manuscript. We also thank Keisuke Yokota and Rie Iida (National Institute of Agrobiological Sciences, Japan) for technical assistance. This work was supported by a grant from the Japanese Program for the Promotion of Basic Research Activities for Innovative Biosciences (to H.I.–A.).

SUPPORTING INFORMATION

Additional Supporting Information may be found in the online version of this article.

Figure S1. Multiple alignment of expansin protein sequences by CLUSTALW.

Figure S2. Root hair-specific expression analysis of *RH101* and *RH102* in response to infection by *Mesorhizobium loti*.

Figure S3. Promoter sequences of *LjEXP7* and *LjEXPA8*.

Figure S4. Histochemical localization of GUS activity in wild-type roots transformed with the *pEpi::GUS*$^{+}$ vector.

Figure S5. Rhizobial infection and nodule organogenesis phenotypes of wild-type roots transformed with the *pEpi::GUS*$^{+}$ vector.

Figure S6. Expression analysis of symbiosis genes in root hairs, stripped roots and whole roots of *Lotus japonicus*.

Figure S7. Rhizobial infection and nodule organogenesis phenotypes of *nup85–2*, *nup133–3*, *castor–4*, *pollux–3* and *ccamk–3* mutant roots transformed with the empty vector.

Figure S8. Rhizobial infection and nodule organogenesis phenotypes of *nfr1–4*, *nfr5–2*, *nsp1–1* and *nsp2–1* mutant roots transformed with the empty vector.

Figure S9. Stacked histograms comparing frequency counts in terms of the number of nodules or bumps per mutant plants transformed with *CCaMK*, *CASTOR*, *POLLUX*, *NUP85* and *NUP133* driven by *pEpi* or *p35S*.

Figure S10. Spontaneous nodulation phenotypes of wild-type roots transformed with *CCaMK*^{T265D} driven by *pEpi* or *p35S*.

Figure S11. Complementation tests of rhizobial infection and nodule organogenesis phenotypes of *nup85–2*, *nup133–3*, *castor–4* and *pollux–3* mutants transformed with the corresponding genes driven by *p35S*.

Figure S12. Stacked histograms comparing frequency counts in terms of the number of nodules or bumps per mutant plant by co-transformation with *CCaMK* under the control of *pEpi* and truncated *CCaMK1–314* or *CCaMK1–340* under the control of *p35S*.

Figure S13. Spontaneous nodule-like structure of the *ccamk–3* mutant by co-transformation with CCaMK under the control of *pEpi* and truncated *CCaMK1–314* under the control of *p35S*.

Figure S14. Complementation tests of rhizobial infection and nodule organogenesis phenotypes of the *cyclops–3* mutant transformed with *CYCLOPS* driven by *pEpi* or *p35S*.

Figure S15. Stacked histograms comparing frequency counts in terms of the number of nodules or bumps per mutant plant transformed with *CYCLOPS*, *NSP1*, *NSP2*, *NFR1* or *NFR5* driven by *pEpi* or *p35S*.

Figure S16. Complementation tests of rhizobial infection and nodule organogenesis phenotypes of *nsp1–1* and *nsp2–1* mutants transformed with the corresponding genes driven by *pEpi* or *p35S*.

Methods S1. Plasmid construction.

Methods S2. RNA isolation from root hairs.

Table S1. Spontaneous nodulation phenotypes.

Table S2. Primer sequences used for construction.

Table S3. Primer sequences used in the expression analysis.

REFERENCES

Ané, J.M., Kiss, G.B., Riely, B.K. *et al.* (2004) *Medicago truncatula DMI1* required for bacterial and fungal symbioses in legumes. *Science*, **303**, 1364–1367.

Arrighi, J.F., Barre, A., Ben Amor, B. *et al.* (2006) The *Medicago truncatula* lysine motif-receptor-like kinase gene family includes *NFP* and new nodule-expressed genes. *Plant Physiol.* **142**, 265–279.

Broghammer, A., Krusell, L., Blaise, M. *et al.* (2012) Legume receptors perceive the rhizobial lipochitin oligosaccharide signal molecules by direct binding. *Proc. Natl Acad. Sci. USA*, **109**, 13859–13864.

Broughton, W.J. and Dilworth, M.J. (1971) Control of leghaemoglobin synthesis in snake beans. *Biochem. J.*, **125**, 1075–1080.

Cho, H.T. and Cosgrove, D.J. (2002) Regulation of root hair initiation and expansin gene expression in Arabidopsis. *Plant Cell*, **14**, 3237–3253.

Cui, H., Levesque, M.P., Vernoux, T., Jung, J.W., Paquette, A.J., Gallagher, K.L., Wang, J.Y., Blilou, I., Scheres, B. and Benfey, P.N. (2007) An evolutionarily conserved mechanism delimiting SHR movement defines a single layer of endodermis in plants. *Science*, **316**, 421–425.

Díaz, C.L., Grønlund, M., Schlaman, H.R.M. and Spaink, H.P. (2005) Induction of hairy roots for symbiotic gene expression studies. In *Lotus japonicus* Handbook (Márguez, A.J., ed.). Dordrecht, The Netherlands: Springer, pp. 261–277.

Flemetakis, E., Kavroulakis, N., Quaedvlieg, N.E., Spaink, H.P., Dimou, M., Roussis, A. and Katinakis, P. (2000) *Lotus japonicus* contains two distinct ENOD40 genes that are expressed in symbiotic, nonsymbiotic, and embryonic tissues. *Mol. Plant Microbe Interact.* **13**, 987–994.

Gleason, C., Chaudhuri, S., Yang, T., Muñoz, A., Poovaiah, B.W. and Oldroyd, G.E. (2006) Nodulation independent of rhizobia induced by a calcium-activated kinase lacking autoinhibition. *Nature*, **441**, 1149–1152.

Gonzalez-Rizzo, S., Crespi, M. and Frugier, F. (2006) The *Medicago truncatula* CRE1 cytokinin receptor regulates lateral root development and early symbiotic interaction with *Sinorhizobium meliloti*. *Plant Cell*, **18**, 2680–2693.

Groth, M., Takeda, N., Perry, J. *et al.* (2010) *NENA*, a *Lotus japonicus* homolog of *Sec13*, is required for rhizodermal infection by arbuscular mycorrhiza fungi and rhizobia but dispensable for cortical endosymbiotic development. *Plant Cell*, **22**, 2509–2526.

Hayashi, T., Banba, M., Shimoda, Y., Kouchi, H., Hayashi, M. and Imaizumi-Anraku, H. (2010) A dominant function of CCaMK in intracellular accommodation of bacterial and fungal endosymbionts. *Plant J.* **63**, 141–154.

Heckmann, A.B., Lombardo, F., Miwa, H., Perry, J.A., Bunnewell, S., Parniske, M., Wang, T.L. and Downie, J.A. (2006) *Lotus japonicus* nodulation requires two GRAS domain regulators, one of which is functionally conserved in a non-legume. *Plant Physiol.* **142**, 1739–1750.

Heckmann, A.B., Sandal, N., Bek, A.S., Madsen, L.H., Jurkiewicz, A., Nielsen, M.W., Tirichine, L. and Stougaard, J. (2011) Cytokinin induction of root nodule primordia in *Lotus japonicus* is regulated by a mechanism operating in the root cortex. *Mol. Plant Microbe Interact.* **24**, 1385–1395.

Hirsch, A.M. (1992) Developmental biology of legume nodulation. *New Phytol.* **122**, 211–237.

Imaizumi-Anraku, H., Takeda, N., Charpentier, M. *et al.* (2005) Plastid proteins crucial for symbiotic fungal and bacterial entry into plant roots. *Nature*, **433**, 527–531.

Kaló, P., Gleason, C., Edwards, A. *et al.* (2005) Nodulation signaling in legumes requires NSP2, a member of the GRAS family of transcriptional regulators. *Science*, **308**, 1786–1789.

Kanamori, N., Madsen, L.H., Radutoiu, S. *et al.* (2006) A nucleoporin is required for induction of Ca^{2+} spiking in legume nodule development and essential for rhizobial and fungal symbiosis. *Proc. Natl Acad. Sci. USA*, **103**, 359–364.

Kim, D.W., Lee, S.H., Choi, S.B., Won, S.K., Heo, Y.K., Cho, M., Park, Y.I. and Cho, H.T. (2006) Functional conservation of a root hair cell-specific *cis*-element in angiosperms with different root hair distribution patterns. *Plant Cell*, **18**, 2958–2970.

Kosuta, S., Held, M., Hossain, M.S. *et al.* (2011) *Lotus japonicus symRK–14* uncouples the cortical and epidermal symbiotic program. *Plant J.* **67**, 929–940.

Kouchi, H., Imaizumi-Anraku, H., Hayashi, M., Hakoyama, T., Nakagawa, T., Umehara, Y., Suganuma, N. and Kawaguchi, M. (2010) How many peas in a pod? Legume genes responsible for mutualistic symbioses underground. *Plant Cell Physiol.* **51**, 1381–1397.

Lévy, J., Bres, C., Geurts, R. *et al.* (2004) A putative Ca^{2+} and calmodulin-dependent protein kinase required for bacterial and fungal symbioses. *Science*, **303**, 1361–1364.

Liao, J., Singh, S., Hossain, M.S. *et al.* (2012) Negative regulation of CCaMK is essential for symbiotic infection. *Plant J.* **72**, 572–584.

Lohar, D.P., Schaff, J.E., Laskey, J.G., Kieber, J.J., Bilyeu, K.D. and Bird, D.M. (2004) Cytokinins play opposite roles in lateral root formation, and nematode and rhizobial symbioses. *Plant J.* **38**, 203–214.

Lohmann, G.V., Shimoda, Y., Nielsen, M.W. *et al.* (2010) Evolution and regulation of the *Lotus japonicus LysM receptor gene* family. *Mol. Plant Microbe Interact.* **23**, 510–521.

Madsen, E.B., Madsen, L.H., Radutoiu, S. *et al.* (2003) A receptor kinase gene of the LysM type is involved in legume perception of rhizobial signals. *Nature*, **425**, 637–640.

Madsen, L.H., Tirichine, L., Jurkiewicz, A., Sullivan, J.T., Heckmann, A.B., Bek, A.S., Ronson, C.W., James, E.K. and Stougaard, J. (2010) The molecular network governing nodule organogenesis and infection in the model legume *Lotus japonicus*. *Nat. Commun.* **1**, 10.

Maekawa, T., Hayashi, M. and Murooka, Y. (2005) Root hair abundant genes *LjRH101* and *LjRH102* encode peroxidase and xyloglucan endotransglycosylase in *Lotus japonicus*. *J. Biosci. Bioeng.* **99**, 84–86.

Maekawa, T., Maekawa-Yoshikawa, M., Takeda, N., Imaizumi-Anraku, H., Murooka, Y. and Hayashi, M. (2009) Gibberellin controls the nodulation signaling pathway in *Lotus japonicus*. *Plant J.* **58**, 183–194.

Marsh, J.F., Rakocevic, A., Mitra, R.M., Brocard, L., Sun, J., Eschstruth, A., Long, S.R., Schultze, M., Ratet, P. and Oldroyd, G.E. (2007) *Medicago truncatula NIN* is essential for rhizobial-independent nodule organogenesis induced by autoactive calcium/calmodulin-dependent protein kinase. *Plant Physiol.* **144**, 324–335.

Miwa, H., Sun, J., Oldroyd, G.E. and Downie, J.A. (2006) Analysis of Nod-factor-induced calcium signaling in root hairs of symbiotically defective mutants of *Lotus japonicus*. *Mol. Plant Microbe Interact.* **19**, 914–923.

Murakami, Y., Miwa, H., Imaizumi-Anraku, H., Kouchi, H., Downie, J.A., Kawaguchi, M. and Kawasaki, S. (2006) Positional cloning identifies *Lotus japonicus* NSP2, a putative transcription factor of the GRAS family, required for *NIN* and *ENOD40* gene expression in nodule initiation. *DNA Res.* **13**, 255–265.

Murray, J.D., Karas, B.J., Sato, S., Tabata, S., Amyot, L. and Szczyglowski, K. (2007) A cytokinin perception mutant colonized by *Rhizobium* in the absence of nodule organogenesis. *Science*, **315**, 101–104.

Oldroyd, G.E. and Downie, A. (2008) Coordinating nodule morphogenesis with rhizobial infection in legume. *Annu. Rev. Plant Biol.* **59**, 519–546.

Parniske, M. (2008) Arbuscular mycorrhiza: the mother of plant root endosymbioses. *Nat. Rev. Microbiol.* **6**, 763–775.

Radutoiu, S., Madsen, L.H., Madsen, E.B. *et al.* (2003) Plant recognition of symbiotic bacteria requires two LysM receptor-like kinases. *Nature*, **425**, 585–592.

Rival, P., de Billy, F., Bono, J.J., Gough, C., Rosenberg, C. and Bensmihen, S. (2012) Epidermal and cortical roles of *NFP* and *DMI3* in coordinating early steps of nodulation in *Medicago truncatula*. *Development*, **139**, 3383–3391.

Saito, K., Yoshikawa, M., Yano, K. *et al.* (2007) NUCLEOPORIN85 is required for calcium spiking, fungal and bacterial symbioses, and seed production in *Lotus japonicus*. *Plant Cell*, **19**, 610–624.

Sandal, N., Petersen, T.R., Murray, J. *et al.* (2006) Genetics of symbiosis in *Lotus japonicus*: recombinant inbred lines, comparative genetic maps,

and map position of 35 symbiotic loci. *Mol. Plant Microbe Interact.* **19**, 80–91.

Schauser, L., Roussis, A., Stiller, J. and Stougaard, J. (1999) A plant regulator controlling development of symbiotic root nodules. *Nature*, **402**, 191–195.

Shimoda, Y., Han, L., Yamazaki, T., Suzuki, R., Hayashi, M. and Imaizumi-Anraku, H. (2012) Rhizobial and fungal symbioses show different requirements for calmodulin binding to calcium calmodulin-dependent protein kinase in *Lotus japonicus*. *Plant Cell*, **24**, 304–321.

Sieberer, B.J., Chabaud, M., Fournier, J., Timmers, A.C. and Barker, D.G. (2012) A switch in Ca^{2+} spiking signature is concomitant with endosymbiotic microbe entry into cortical root cells of *Medicago truncatula*. *Plant J.* **69**, 822–830.

Singh, S. and Parniske, M. (2012) Activation of calcium- and calmodulin-dependent protein kinase (CCaMK), the central regulator of plant root endosymbiosis. *Curr. Opin. Plant Biol.* **15**, 444–453.

Smit, P., Raedts, J., Portyanko, V., Debellé, F., Gough, C., Bisseling, T. and Geurts, R. (2005) NSP1 of the GRAS protein family is essential for rhizobial Nod factor-induced transcription. *Science*, **308**, 1789–1791.

Stracke, S., Kistner, C., Yoshida, S. *et al.* (2002) A plant receptor-like kinase required for both bacterial and fungal symbiosis. *Nature*, **417**, 959–962.

Timmers, A.C., Auriac, M.C., de Billy, F. and Truchet, G. (1998) Nod factor internalization and microtubular cytoskeleton changes occur concomitantly during nodule differentiation in alfalfa. *Development*, **125**, 339–349.

Tirichine, L., Imaizumi-Anraku, H., Yoshida, S. *et al.* (2006) Deregulation of a Ca^{2+}/calmodulin-dependent kinase leads to spontaneous nodule development. *Nature*, **441**, 1153–1156.

Tirichine, L., Sandal, N., Madsen, L.H., Radutoiu, S., Albrektsen, A.S., Sato, S., Asamizu, E., Tabata, S. and Stougaard, J. (2007) A gain-of-function mutation in a cytokinin receptor triggers spontaneous root nodule organogenesis. *Science*, **315**, 104–107.

Yano, K., Yoshida, S., Müller, J. *et al.* (2008) CYCLOPS, a mediator of symbiotic intracellular accommodation. *Proc. Natl Acad. Sci. USA*, **105**, 20540–20545.

